Strain Pattern in Supercooled Liquids

Bernd Illing,[1] Sebastian Fritschi,[1] David Hajnal,[2,*] Christian Klix,[1] Peter Keim,[1] and Matthias Fuchs[1]

[1]*University of Konstanz, D-78457 Konstanz, Germany*
[2]*Johannes Gutenberg-University Mainz, D-55099 Mainz, Germany*

Investigations of strain correlations at the glass transition reveal unexpected phenomena. The shear strain fluctuations show an Eshelby-strain pattern [$\sim \cos(4\theta)/r^2$], characteristic of elastic response, even in liquids, at long times. We address this using a mode-coupling theory for the strain fluctuations in supercooled liquids and data from both video microscopy of a two-dimensional colloidal glass former and simulations of Brownian hard disks. We show that the long-ranged and long-lived strain signatures follow a scaling law valid close to the glass transition. For large enough viscosities, the Eshelby-strain pattern is visible even on time scales longer than the structural relaxation time τ and after the shear modulus has relaxed to zero.

Glasses behave like isotropic elastic solids under external loads. Their strain fields are long ranged as captured in elasticity theory. Considering appropriate boundary conditions, Eshelby obtained the elastic strain field surrounding an isolated local deformation [1], which is also the basis for modern theories of plasticity in disordered solids [2]: plastic deformation proceeds via localized irreversible rearrangements coupled by elastic strain fields.

While the relevance of strain in glass at low temperatures originates in the breaking of translational symmetry underlying solidification [3], the proper understanding of the evolution of strains at the crossover from a metastable glass to a supercooled liquid remains an old [4] yet open topic [5]. The concept of plastic events, which are elastically coupled, has emerged as one candidate rooted in the theory of solids that aims to capture the glass transition from low temperatures. It suggests that "supercooled liquids are solids that flow" [6] and focuses on strain fluctuations and their correlations to probe plastic flow.

Lemaître and colleagues found evidence for this concept in molecular dynamics simulations of two-dimensional Lennard-Jones mixtures: they observed persistent long-ranged strain fluctuations in supercooled liquid states [7]. Because the time over which strains were accumulated exceeds the structural relaxation time τ of the liquid, observable elastic stresses have decayed. The observation of spatial dependencies exhibiting a far-field Eshelby-strain pattern thus cannot be a simple consequence of elasticity. It suggests that particle rearrangements in a fluid interact over large distances via strains likely in an underlying elastic structure, the "inherent states" characterizing the potential energy landscape [8].

Strain patterns have been observed experimentally, but not yet in quiescent supercooled liquids. An anisotropic decay of strain was found in a 3D colloidal hard sphere glass under steady shear [9], in 2D simulations [10,11]

where long range correlations enhance phonon scattering [12], and in granular matter [13]. Eshelby patterns are reported in 2D flowing emulsions [14] and in a 3D colloidal hard sphere glass, where they appear under shear and thermally induced in a quiescent state [15]. They are also present in 2D soft hexagonal crystals with dipolar interaction [16]. Simulations revealed Eshelby patterns in a 2D flowing foam [17] and in a glass-forming mixture under shear [18]. For a monodisperse fluid system in 2D of particles with screened Coulomb interaction, these patterns were observed in the short time regime due to the high frequency shear modulus [19].

In this Letter, we present the first experimental evidence for Eshelby-like strain patterns in quiescent supercooled liquids and provide a theoretical description rooted in theories of liquid dynamics. This establishes the dissipative transport mechanism leading to long-ranged strain fluctuations and identifies the spatial and temporal window where they can be observed in supercooled states.

Monolayers of binary mixtures of dipolar colloids have emerged as a model system for the study of the glass transition by video microscopy [20]. The dipolar interaction between colloids can be tuned by an external magnetic field and the interaction parameter Γ (magnetic over thermal energy) is precisely known; it may be considered a dimensionless inverse temperature. Strain fields can be determined from the particle trajectories in crystalline [21] and amorphous [22] solids, and the shear modulus μ could be measured [23]. Solutions of the mode-coupling theory (MCT) provide theoretical results for the glass transition [24].

The dynamics of the system shall be captured in the average correlation of accumulated strains at two different locations $\mathbf{r}_{1,2}$, $C_{\alpha\beta\gamma\delta}(\mathbf{r}_1, \mathbf{r}_2, t) = \langle \Delta\varepsilon_{\alpha\beta}(\mathbf{r}_1, t)\Delta\varepsilon_{\gamma\delta}(\mathbf{r}_2, t) \rangle$. Here, $\varepsilon_{\alpha\beta}$ is the familiar (linearized) strain tensor with spatial indices $\alpha, \beta \in \{1, 2\}$ in two dimensions. It is

obtained from the differences of particle positions accumulated over the time span t [25]. Equilibrium averaging is done with the Gibbs-Boltzmann distribution [26], and time-translational invariance of the system is assumed and experimentally achieved by careful equilibration for several days up to weeks in between the measurements at different temperatures (Γ). In a homogeneous system, the correlations depend on the distance $\mathbf{r} = \mathbf{r}_2 - \mathbf{r}_1$ only. In an isotropic system, the fourth rank tensor can be reduced to two independent functions related to compressional and shear deformations. Following Ref. [7], we focus on the transverse element $C_{xy}(\mathbf{r}, t) = C_{xyxy}(\mathbf{r}, t)$; more details can be found in the Supplemental Material [27].

Figure 1 shows the measured transversal strain correlations for a glass and a fluid state. They were obtained using video microscopy on a binary colloidal monolayer [23] following the analysis introduced in Ref. [25]. A brief introduction of the experimental setup can be found in the
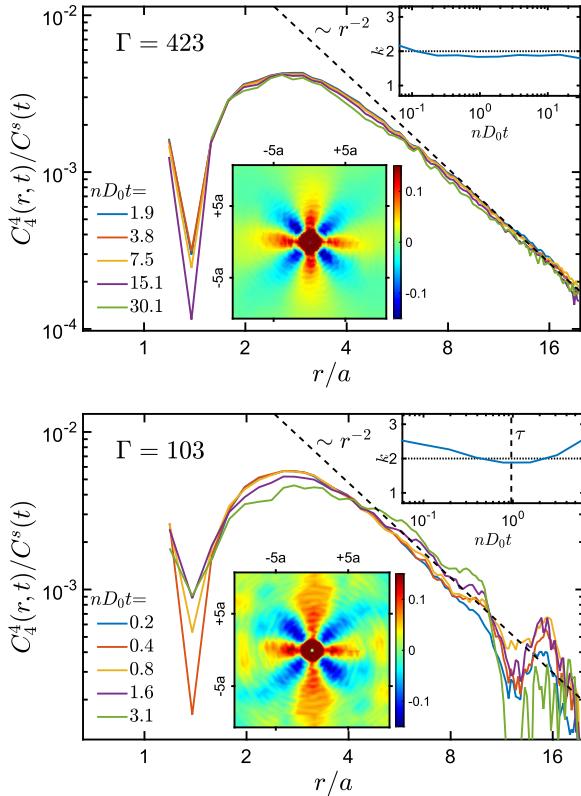
FIG. 1. Experimental rescaled strain correlation data for a glass (upper panel, $\Gamma = 423$) and a fluid (lower panel, $\Gamma = 103$) state at different times (see legends). The spherical harmonic strain correlation functions $C_4^4(r, t)/C^s(t)$ are rescaled to overlap in the far-field power-law decay. The main panels show the $1/r^k$ power-law decay (dashed black), with the exponent $k = 2$ varying little with time (upper insets). The contour plots (lower insets) of the long-time limit of $C_{xy}(\mathbf{r}, t)/C_{xy}(\mathbf{r} = 0, t)$ illustrate the corresponding $\cos(4\theta)$ symmetry; The Eshelby patterns are shown at $nD_0t = 30.1$ (glass) and $nD_0t = 3.1 > nD_0\tau$ (fluid), respectively.

Supplemental Material [27] while an elaborate discussion is given in Ref. [31]. Time is given in reduced units with D_0n the rate for the (unhindered) diffusion of a particle over the average particle separation $a = 1/\sqrt{n}$, where n is the particle density; D_0 is the dilute diffusion coefficient. One notices the angular dependence of the far-field strain, which Eshelby obtained for the elastic distortion around a localized disturbance at the origin [1,32]:

$$C_{xy}(\mathbf{r}, t) \to \cos(4\theta) \frac{C^s(t)}{4\pi nr^2}, \quad \text{for } r \gg a. \quad (1)$$

Four lobes of maximal intensity alternate with four lobes of minimal intensity. The appropriate spherical harmonics projection $C_4^4(r, t) = (1/\pi) \int_0^{2\pi} d\theta \cos(4\theta) C_{xy}(\mathbf{r}, t)$ decays slowly at large separations $r \gg a$, with a power law $C_4^4 \propto r^{-k}$ of exponent $k = 2$ (see the dashed line in Fig. 1). This is the classical result from continuum mechanics and linear response theory (viz., the fluctuation dissipation theorem) for the strain fluctuations in an isotropic solid. We find that it holds for times beyond the short time local dynamics (viz., $nD_0t \gtrsim 1$) and for distances r larger than the average particle separation a. The algebraic decay of hexadecupolar symmetry follows from the fundamental equation of elastostatics, which predicts for the amplitude of the algebraic decay $C^s(t \to \infty) = 2k_BTn(1/\mu - 1/\mu^\parallel)$. Here, the elasticity seen in (volume-preserving) strain-deformations is the hallmark of a solid and results from a finite shear modulus μ. The longitudinal modulus $\mu^\parallel$, which would be present in a fluid also, gives a (small) correction in C_{xy}. The observation of a finite shear rigidity is consistent with the interpretation that the colloidal layer is in a solid state at low temperatures, viz., $\Gamma > \Gamma_g \approx 200$, where Γ_g is the inverse dimensionless glass transition temperature obtained from the discontinuity in the elastic moduli [23].

The measured spatial correlations of the strains persist in fluid states at $\Gamma = 103 < \Gamma_g$. At this temperature, approximately 2 times higher than the glass transition temperature, the averaged strain fluctuations exhibit spatial correlations reminiscent of solids even for times far larger than the structural relaxation time τ. The upper inset in Fig. 1 at $\Gamma = 103$ compares the times t where Eq. (1) holds with τ. It is estimated from the decay of the density correlations with the wavelength of the average particle separation [27]. The relaxation time τ also characterizes the decay to zero of the shear stress autocorrelation function, which indicates that the fluid cannot sustain elastic shear stresses for such long times [33]. Thus, we experimentally recover the intriguing observation by Lemaître and colleagues that solidlike Eshelby strain fields survive in supercooled fluids even though density and stress correlations are fluidlike.

In order to understand the spatial strain correlations at the glass transition, we turn to microscopic quantities, which provide insights into fluid and solid states. The transversal

collective mean-squared displacement (TCMSD) function $C^\perp(q,t) = \langle \Delta \mathbf{u}_\mathbf{q}^{\perp*}(t) \Delta \mathbf{u}_\mathbf{q}^\perp(t) \rangle$ can be obtained from the particles' displacements accumulated in the time interval t [22]. The spatial Fourier transformation possible in homogeneous systems allows us to focus on shear fluctuations perpendicular to the wave vector $\mathbf{q}$. The TCMSD may be considered a collective and spatially resolved generalization of the single particle mean-squared displacement familiar from liquid dynamics [26].

The transverse strain correlation function is given by the inverse Fourier transformation: $C_{xy}(\mathbf{r},t) = \mathrm{FT}^{-1}\{[(q_x^2 + q_y^2/4) - (q_x^2 q_y^2/q^2)]C^\perp(q,t)]\}(\mathbf{r})$, where the $\mathbf{q}$-dependent factors arise as strain is the symmetrized gradient of the displacement field in linear order [34]. For simplicity of presentation, we assume an incompressible system from now on, neglecting a longitudinal collective mean-squared displacement $C^\parallel(q,t)$, and relegate the complete theoretical analysis of compressible systems to the Supplemental Material [27].

The overdamped equations of motion of the (complete tensorial) collective mean-squared displacement were given in Ref. [22]. They rest on (i) the link between the displacement and velocity fluctuations $\dot{\mathbf{u}}_q = \mathbf{v}_q$ presumed valid in fluid and solid states [35], and on (ii) results for velocity correlations obtained by liquid theory [26]. Figure 2 shows typical curves for the TCMSD numerically obtained employing approximations familiar from MCT in order to evaluate the arising memory kernels [27]. The calculation mimics a two-dimensional one-component system of dipolar Brownian particles, which undergoes a glass transition at $\Gamma_g^{\mathrm{MCT}} = 115$ [24,37]. The curves exhibit
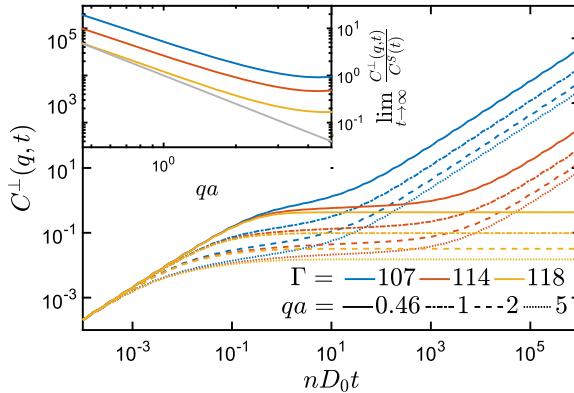
FIG. 2. Transversal collective mean-squared displacements $C^\perp(q,t)$ from MCT for various wave vectors q as labeled and for three different values of Γ. While $\Gamma = 107$ and 114 are fluid states, $\Gamma = 118$ is a glass in this one-component dipolar system. The inset shows that for wave vectors $qa \ll 1$ the $1/q^2$ behavior (gray solid line) predicted by the generalized hydrodynamics result $C_{GH}^\perp(q,t) \to C^s(t)/q^2$ from Eq. (3) is approached at long times for both the glass and fluid. Since the three curves collapse for $qa \ll 1$ the fluid curves are shifted by a factor of 2 and 4, respectively, for visibility.

a scaling limit of generalized hydrodynamics for small wave vectors, which is of central interest in order to obtain the far-field strain behavior.

The generalized hydrodynamics appropriate in supercooled fluids is obtained from taking the limit of long wavelength fluctuations $qa \ll 1$ and keeping the possibility for slow dynamics [39]. Our result, obtained within the Zwanzig-Mori projection operator formalism, describes initially diffusive particle displacements growing linearly in time (with D_0 the dilute diffusion coefficient and the friction coefficient $\zeta_0 = k_B T/D_0$). With increasing time the diffusive displacements get hindered by interactions captured in a retarded friction kernel:

$$C_{\mathrm{GH}}^\perp(q,t) + \frac{q^2}{\zeta_0 n} \int_0^t dt' G^\perp(t - t') C_{\mathrm{GH}}^\perp(q,t') = 2D_0 t, \quad (2)$$

where the subscript GH stands for generalized hydrodynamics. The memory kernel contains the potential shear stresses: $G^\perp(t) = (n/k_B T)\langle \sigma_\perp(t_Q)^* \sigma_\perp \rangle$. Its prefactor q^2 results from Newton's second law, that forces are transmitted among the particles and sum up to zero in total. $G^\perp(t)$ is familiar from the theory of transversal momentum fluctuations in liquids, and its integral gives the shear viscosity according to the Green-Kubo relation [26]: $\eta = \int_0^\infty dt G^\perp(t)$. It differs from the stress autocorrelation function in a solid [40].

The equation of motion for the transversal collective mean-squared displacements contains a length L defined via $(qL)^2 = (q^2\eta/n\zeta_0)$, which determines the behavior at long times [41]. In the normal hydrodynamic description of a liquid, the limit of a small wave vector is taken, which leads to $qL \ll 1$. Then, the displacements grow diffusively for all times, $C_{\mathrm{GH}}^\perp(q \ll 1/L, t) = 2D_0 t$, and the strain correlation function $C_{xy}(\mathbf{r},t)$ decays on local distances. Not surprisingly, an equilibrium liquid does not support long-ranged strain correlations as present in elastic systems. The crossover to simple hydrodynamics happens at $q < 1/L$, with L of the order of the average particle distance a in low-viscous fluids [42]: $L/a = \sqrt{\eta/(\zeta_0 na^2)}$ (which is $\sqrt{\eta/\zeta_0}$ in two dimensions). This wave vector also limits the range where transversal sound waves are seen in supercooled molecular systems [43,44]. In a glass, strain fluctuations are tested at times t shorter than τ before the stresses have relaxed. Then, the shear stress memory kernel takes the value of the shear modulus μ [22], and the variance of the displacements increases with wave vector like a power law: $C_{\mathrm{GH}}^\perp(q, t \ll \tau) = (2k_B Tn/\mu q^2)$. The small-$q$ divergence of the variance of the displacements is the origin of the far-field power law in Eshelby's result. Equation (1) holds with $C^s(t) = 2k_B Tn/\mu$.

The increase of the viscosity opens an additional spatiotemporal window, where the shear modulus has decayed to zero, yet the displacements still diverge

with q^{-2}. This "supercooled liquid" regime is characterized by $t \gg \tau$ and $qL \gg 1$, which requires high values of the viscosity. Then, the TCMSD obeys $C_{\mathrm{GH}}^{\perp}(q \gg 1/L, t \gg \tau) = (2k_BTn/\eta q^2)t$, and the strain correlation function exhibits the spatial behavior reminiscent of solidlike behavior, $C_{xy}(\mathbf{r}, t) \to \cos 4\theta (2k_BTt/\eta r^2)$. Yet, the coefficient of the spatial power law is viscous and not elastic. The long-ranged correlation of strains arises from momentum conservation during the particle interactions, which causes the slow collective transport of momentum in the viscoelastic particle system to dominate over the local friction intrinsic in the Langevin description [45]: $(qL)^2 = (q^2\eta/n)/(\zeta_0) \gg 1$.

The glass and supercooled regimes of the strain fluctuations can be summarized in a scaling law [47]. The coefficient $C^s(t)$ of the far-field strain decay in Eq. (1) can be obtained from a limiting solution of Eq. (2) valid for $qL \gg 1$ and $tD_0n \gg 1$ in incompressible systems:

$$C_{\mathrm{GH}}^{\perp}(q, t) \to \frac{C^s(t)}{q^2} \quad \text{with} \quad C^s(t) \to \begin{cases} \dfrac{2k_BTn}{\mu}, & t \ll \tau, \\[2mm] \dfrac{2k_BTnt}{\eta}, & t \gg \tau. \end{cases}$$
$$(3)$$

The equation for $C^s(t)$ follows from Eq. (2) by neglecting the first term. The ansatz of an exponentially decaying memory kernel $G^{\perp} = \mu e^{-t/\tau}$ would capture both asymptotes on the right-hand side of Eq. (3): in analogy to a Maxwell fluid under load, μ would appear for short times and η/t for long ones.

Figure 3 contains the measured $C^s(t)$ obtained from the real-space analysis considering the far-field power-law decay of the strain correlations shown in Fig. 1 [27]. Additional data sets around the glass transition (inverse) temperature $\Gamma_g \approx 200$ are added. In the lower panel, $C^s(t)$ data obtained identically from Brownian dynamics (BD) simulations of binary hard disks are shown. The system's glass transition packing fraction lies at $\phi_g \approx 0.795$ [49]. The measured data from experiment and simulation qualitatively agree and exhibit the predicted behaviors. Over a time window increasing when approaching the glass transition, the far-field amplitude $C^s(t)$ is arrested on a constant value as corresponds to elastic solidlike behavior. The elastic moduli determined independently closely match the plateau values during the intermediate time window. In fluid states, the far-field amplitude increases for long times asymptotically linearly in time with a prefactor given by the inverse viscosity, or equivalently the final relaxation time τ. Rescaling $C^s(t)$ during this final process using τ obtained *a priori* from the density correlation functions (see the Supplemental Material [27]) gives a satisfactory collapse of the curves in fluid states, see the insets of Fig. 3. The BD data would collapse far better if replotted versus nD_Lt (not shown), where D_L is the long-time self-diffusion
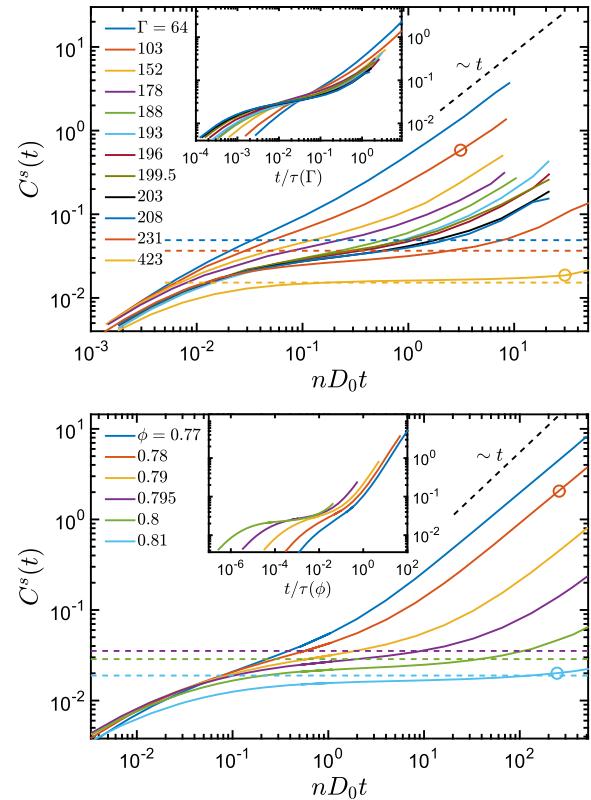
FIG. 3. Amplitude function $C^s(t)$ of the far-field power-law decay of transversal strain correlations given in Eq. (1). It gives the strength of the algebraic $1/r^2$ power-law decay with $\cos(4\theta)$ symmetry in $C_{xy}(\mathbf{r}, t)$, which holds for $a \ll r \ll L$ according to Eq. (3). The upper panel gives data measured in the colloidal layers, the lower panel gives the corresponding data measured by BD simulations in a binary mixture of hard disks [27]. The legends give the inverse temperatures Γ or the packing fractions ϕ spanning from the fluid to glass states. The circles mark the times where Eshelby-strain patterns are shown in the inset of Fig. 1 (and Fig. 5 in the Supplemental Material [27]). The dashed lines give the elastic limits $C^s(t \to \infty) = 2k_BTn(1/\mu - 1/\mu^{\parallel})$ with the moduli obtained from the dispersion relations following Ref. [22]. The insets show the asymptotic collapse of the fluid curves when plotted versus the rescaled time t/τ with the final relaxation times τ obtained from density correlation functions [27].

coefficient. This may indicate that the strain fluctuations decouple from the structural relaxation as is familiar for diffusion, which is often taken as an indication for heterogeneous dynamics [50].

In summary, we have shown that hexadecupolar Eshelby-strain correlations, which are reminiscent of standard elastic behavior, can also be detected in an experiment for a supercooled fluid when the shear elasticity has already decayed to zero in the long-time limit. An analysis of the retarded averaged strain fluctuation functions within the framework of mode-coupling theory can explain this: for sufficiently large viscosities an additional spatiotemporal window opens where correlated displacements diverge with length scales squared (q^{-2}) while elastic correlations have

already decayed. The origin of the long-ranged strain fluctuations is the conservation of momentum in the particle interactions. This derivation within the generalized hydrodynamics of supercooled liquids opens the perspective to connect to the theories of plastic flow in low-temperature glasses. For example, the connection of our viscoelastic scaling law to inherent structures remains to be established and promises insights into the dynamics on the potential energy landscape at high temperatures [51]. While for long times and large distances, flow and elastic processes cause similar patterns, differences might be detectable at short scales. Our theoretical results in Fourier space hold in two and three dimensions, and rationalize data from colloidal layers, even though computer simulations of single particle motion indicated that localization in two-dimensional glasses is rather weak [52]. Accordingly, our simulations require large systems in order to observe the far-field behavior.

---

[*] Present Address: BASF SE, Carl-Bosch-Strasse 38, D-67056 Ludwigshafen, Germany.

[1] J. Eshelby, The determination of the elastic field of an ellipsoidal inclusion, and related problems, Proc. R. Soc. A **241**, 376 (1957).

[2] J.-L. Barrat and A. Lemaître, *Dynamical Heterogeneities in Glasses, Colloids and Granular Media* (Oxford University Press, New York, 2011), pp. 264–297.

[3] P. C. Martin, O. Parodi, and P. S. Pershan, Unified hydrodynamic theory for crystals, liquid crystals, and normal fluids, Phys. Rev. A **6**, 2401 (1972).

[4] M. Goldstein, Viscous liquids and the glass transition: A potential energy barrier picture, J. Chem. Phys. **51**, 3728 (1969).

[5] E. Flenner and G. Szamel, Long-Range Spatial Correlations of Particle Displacements and the Emergence of Elasticity, Phys. Rev. Lett. **114**, 025501 (2015).

[6] J. C. Dyre, Colloquium: The glass transition and elastic models of glass-forming liquids, Rev. Mod. Phys. **78**, 953 (2006).

[7] J. Chattoraj and A. Lemaître, Elastic Signature of Flow Events in Supercooled Liquids Under Shear, Phys. Rev. Lett. **111**, 066001 (2013).

[8] A. Lemaître, Structural Relaxation is a Scale-Free Process, Phys. Rev. Lett. **113**, 245702 (2014).

[9] V. Chikkadi, S. Mandal, B. Nienhuis, D. Raabe, F. Varnik, and P. Schall, Shear-induced anisotropic decay of correlations in hard-sphere colloidal glasses, Europhys. Lett. **100**, 56001 (2012).

[10] F. Varnik, S. Mandal, V. Chikkadi, D. Denisov, P. Olsson, D. Vagberg, D. Raabe, and P. Schall, Correlations of plasticity in sheared glasses, Phys. Rev. E **89**, 040301 (2014).

[11] A. Le Bouil, A. Amon, S. McNamara, and J. Crassous, Emergence of Cooperativity in Plasticity of Soft Glassy Materials, Phys. Rev. Lett. **112**, 246001 (2014).

[12] S. Gelin, H. Tanaka, and A. Lemaître, Anomalous phonon scattering and elastic correlations in amorphous solids, Nat. Mater., doi: 10.1038/nmat4736 (2016).

[13] D. V. Denisov, K. A. Lörincz, J. T. Uhl, K. A. Dahmen, and P. Schall, Universality of slip avalanches in flowing granular matter, Nat. Commun. **7**, 10641 (2016).

[14] K. W. Desmond and E. R. Weeks, Measurement of Stress Redistribution in Flowing Emulsions, Phys. Rev. Lett. **115**, 098302 (2015).

[15] K. E. Jensen, D. A. Weitz, and F. Spaepen, Local shear transformations in deformed and quiescent hard-sphere colloidal glasses, Phys. Rev. E **90**, 042305 (2014).

[16] K. Franzrahe, P. Keim, G. Maret, P. Nielaba, and S. Sengupta, Nonlocal elastic compliance for soft solids: Theory, simulations, and experiments, Phys. Rev. E **78**, 026106 (2008).

[17] V. Chikkadi, E. Woldhuis, M. v. Hecke, and P. Schall, Correlations of strain and plasticity in a flowing foam, Europhys. Lett. **112**, 36004 (2015).

[18] A. Nicolas, J. Rottler, and J.-L. Barrat, Spatiotemporal correlations between plastic events in the shear flow of athermal amorphous solids, Eur. Phys. J. E **37**, 50 (2014).

[19] B. Wu, T. Iwashita, and T. Egami, Anisotropic stress correlations in two-dimensional liquids, Phys. Rev. E **91**, 032301 (2015).

[20] H. König, R. Hund, K. Zahn, and G. Maret, Experimental realization of a model glass former in 2D, Eur. Phys. J. E **18**, 287 (2005).

[21] P. Keim, G. Maret, U. Herz, and H. H. von Grünberg, Harmonic Lattice Behavior of Two-Dimensional Colloidal Crystals, Phys. Rev. Lett. **92**, 215504 (2004).

[22] C. L. Klix, F. Ebert, F. Weysser, M. Fuchs, G. Maret, and P. Keim, Glass Elasticity from Particle Trajectories, Phys. Rev. Lett. **109**, 178301 (2012).

[23] C. L. Klix, G. Maret, and P. Keim, Discontinuous Shear Modulus Determines the Glass Transition Temperature, Phys. Rev. X **5**, 041033 (2015).

[24] D. Hajnal, M. Oettel, and R. Schilling, Glass transition of binary mixtures of dipolar particles in two dimensions, J. Non-Cryst. Solids **357**, 302 (2011).

[25] I. Goldhirsch and C. Goldenberg, On the microscopic foundations of elasticity, Eur. Phys. J. E **9**, 245 (2002).

[26] J.-P. Hansen and I. R. McDonald, *Theory of Simple Liquids*, 2nd ed. (Academic Press, London, 1986).

[27] See Supplemental Material at http://link.aps.org/supplemental/10.1103/PhysRevLett.117.208002 for additional details of theory, simulation, and experiment, which includes Refs. [28–30].

[28] A. Scala, Th. Voigtmann, and C. De Michele, Event-driven brownian dynamics for hard spheres, J. Chem. Phys. **126**, 134109 (2007).

[29] O. Henrich, F. Weysser, M. E. Cates, and M. Fuchs, Hard discs under steady shear: comparison of brownian dynamics simulations and mode coupling theory, Phil. Trans. R. Soc. A **367**, 5033 (2009).

[30] B. J. Alder, D. M. Gass, and T. E. Wainwright, Studies in molecular dynamics. VIII. The transport coefficients for a hard-sphere fluid, J. Chem. Phys. **53**, 3813 (1970).

[31] F. Ebert, P. Dillmann, G. Maret, and P. Keim, The experimental realization of a two-dimensional colloidal system, Rev. Sci. Instrum. **80**, 083902 (2009).

[32] G. Picard, A. Ajdari, F. Lequeux, and L. Bocquet, Elastic consequences of a single plastic event: A step towards the microscopic modeling of the flow of yield stress fluids, Eur. Phys. J. E **15**, 371 (2004).

[33] While noise on the measured interaction forces prevented us from obtaining the shear stress autocorrelation functions in experiment, the BD simulations provide τ from density and stress correlations and show the validity of Eq. (1) up to $nD_0 t \approx 500 > 40\tau$ (for $\phi = 0.78$) [27].

[34] J. Salencon, *Handbook of Continuum Mechanics: General Concepts, Thermoelasticity* (Springer-Verlag, Berlin, 2001).

[35] In crystals, the time derivative of the displacement field contains the velocity but also a dissipative (isothermal) coupling to the deviatoric stress field: $\partial_t \mathbf{u}(\mathbf{r}, t) = \mathbf{v}(\mathbf{r}, t) - \zeta \nabla (\boldsymbol{\sigma}(\mathbf{r}, t) - p\mathbf{1})$ [3]; see Ref. [36] concerning displacements as excitations from quasiequilibrium positions.

[36] G. Szamel and E. Flenner, Emergence of Long-Range Correlations and Rigidity at the Dynamic Glass Transition, Phys. Rev. Lett. **107**, 105505 (2011).

[37] The difference of Γ_g between MCT and experiment rests partly on the number of components, but also on the known aspect of MCT to overestimate the tendency to vitrification [24,38].

[38] W. Götze, *Complex Dynamics of Glass-Forming Liquids, A Mode-Coupling Theory* (Oxford University Press, New York, 2009).

[39] W. Götze and A. Latz, Generalised constitutive equations for glassy systems, J. Phys. Condens. Matter **1**, 4169 (1989).

[40] J. P. Wittmer, H. Xu, and J. Baschnagel, Shear-stress relaxation and ensemble transformation of shear-stress autocorrelation functions, Phys. Rev. E **91**, 022107 (2015).

[41] At long times, a Markovian approximation to the memory kernel is valid, which explains the occurrence of the shear viscosity in L.

[42] Note that this crossover is outside the wave vector grid used in the MCT numerical calculations of Fig. 2.

[43] R. Ahluwalia and S. P. Das, Growing length scale related to the solidlike behavior in a supercooled liquid, Phys. Rev. E **57**, 5771 (1998).

[44] D. H. Torchinsky, J. A. Johnson, and K. A. Nelson, α-scale decoupling of the mechanical relaxation and diverging shear wave propagation length scale in triphenylphosphite, J. Chem. Phys. **136**, 174509 (2012).

[45] Connecting the shear modulus to a transversal sound velocity via $\mu = mnv_\perp^2$ for mass density mn, the length becomes $L^2 = v_\perp^2 (m/\zeta)\tau$. It asymptotically exceeds the solidity length introduced by Dyre ($L^4 = a^3 v_\parallel \tau$) [46], which describes finer scales than those accessible in our generalized hydrodynamics approach.

[46] J. C. Dyre, Solidity of viscous liquids, Phys. Rev. E **59**, 2458 (1999).

[47] MCT actually predicts also a second β-scaling law beyond the α-scaling law of Eq. (3) [38] and anomalous vibrational excitations [48].

[48] W. Götze and M. R. Mayr, Evolution of vibrational excitations in glassy systems, Phys. Rev. E **61**, 587 (2000).

[49] F. Weysser and D. Hajnal, Tests of mode-coupling theory in two dimensions, Phys. Rev. E **83**, 041503 (2011).

[50] T. Rizzo and T. Voigtmann, Qualitative features at the glass crossover, Europhys. Lett. **111**, 56008 (2015).

[51] S. Chowdhury, S. Abraham, T. Hudson, and P. Harrowell, Long range stress correlations in the inherent structures of liquids at rest, J. Chem. Phys. **144**, 124508 (2016).

[52] E. Flenner and G. Szamel, Fundamental differences between glassy dynamics in two and three dimensions, Nat. Commun. **6**, 7392 (2015).